A Manganese (II) Dimer Bearing the Reduced Derivatives of Nitronyl Nitroxides

Dimitris I. Alexandropoulos,[1] Fanmiao Kong,[1] Federico Lombardi,[1] Peter N. Horton,[2] and Lapo Bogani*[1]

[1]Department of Materials, University of Oxford16 Parks Road, OX1 3PH, Oxford, UK.

[2]National Crystallography Service, School of Chemistry, University of Southampton, Southampton, UK

Abstract

We report the synthesis, magnetic and conducting properties of a new manganese complex $[Mn^{II}(hfac)_2(IMHPhOPh)]_2[Mn^{II}(hfac)_3](IMH_2PhOPh)$ (**1**), containing the reduced forms (IMHPhOPh and IMH_2PhOPh) of the NIT-PhOPh radical (NIT-PhOPh = 2,4‘-benzoxo-4,4,5,5-tetramethylimidazoline-1-oxyl-3-oxide). Direct current magnetic susceptibility studies revealed the presence of weak antiferromagnetic exchange interactions between the metal ions, within the $[Mn^{II}(hfac)_2(IMHPhOPh)]_2$ unit. The EPR spectra of **1** exhibit simultaneous contributions of both the monomeric $[Mn^{II}(hfac)_3]$ and dimeric $[Mn^{II}(hfac)_2(IMHPhOPh)]_2$ species. Conductivity measurements shown that the electrical conduction of **1** is dominated by Ohm’s law, with a conductance value of $1.3(6) \times 10^{-9}$ S/cm.

1. Introduction

Manganese coordination chemistry has been of great interest over the last decades, owing to the applications of manganese complexes in various fields including molecular magnetism[1] and bioinorganic chemistry.[2] In the latter case, the unique biomimetic and biocatalytic role of

manganese complexes is manifested by the presence of a Mn_4Ca cluster in the active site of photosystem II in green plants and algae, which catalyzes the light driven water oxidation to dioxygen.[2b] On the other hand, polynuclear manganese compounds are known to behave as high-spin molecules and/or single molecule magnets (SMMs), since they often possess a large number of unpaired electrons and magnetic anisotropy, arising from the Jahn Teller distortion of Mn^{III} ions. Electron paramagnetic resonance (EPR) spectroscopy has played a crucial role in the determination of the electronic structures of manganese containing complexes in both biological and magnetic systems.[3] For example, detailed information about the chemical environment of manganese complexes in metalloenzymes can be obtained by EPR studies, providing valuable information about the type and the mechanism of the chemical reactions that they are involved.[4] In addition, EPR spectroscopy offers the potential of directly probing the spin levels in magnetic systems and thus its use is still fundamental for understanding the nature of slow magnetic relaxation in transition metal SMMs.[5]

SMMs are species that can exhibit slow magnetization relaxation, due to a molecular origin, below a characteristic blocking temperature.[1g] Their molecular characteristics also offers the potential for use in quantum computing,[6] spintronics[7] and high-density memory storage devices[7] with unrivaled speeds. For transition metal SMMs, the energy barrier to magnetization reversal (U) is given by $S^2 |D|$ or $(S^2 - 1/4)|D|$ for integer and half integer spin systems, respectively, where D is the zero-field splitting parameter.[1g] After the discovery of the first SMM, $[Mn_{12}O_{12}(OAc)_{16}(H_2O)_4]$ $(Mn_{12}OAc)$[1b], much effort has been directed at the isolation of polynuclear transition metal complexes based on the pivotal idea that an increase of metal nuclearity would maximize the spin ground state and magnetic anisotropy of the compounds.[1c, 1g, 8] However, an important parameter that also need to be considered in the design of new SMMs is

the exchange coupling constant, *J*, which is related with the energy separation between the spin group state and the exited states. To that end the metal-radical approach has been developed, in which organic radicals are used as bridging ligands between metal centers, thus, leading to stronger direct magnetic coupling as compared to the indirect super-exchange interactions observed in the case of diamagnetic linkers.[9]

Nitronyl nitroxides[10] are a versatile class of stable free radicals that have been widely used as ligands for the design of molecular nanomagnets. They possess a general formula of NIT-R, comprising at least one 2-(40-R)-4,4,5,5-tetramethylimidazoline-1-oxyl-3-oxide unit (NIT) in which an additional -R functional group can be added.[11] The two -NO groups of NIT-R radicals are chemically equivalent and can coordinate to metal ions while additional coordinating groups can be introduced through the -R substituent, resulting in the formation of zero-dimensional metal complexes of various nuclearities as well as extended solids of dimensionalities spanning from one to three.[12] Magnetically, NIT-R radicals possess one unpaired electron which is mainly delocalized over the π* orbitals of the two -NO groups and, upon coordination, it can be in direct contact with the metal spin carriers, giving rise to strong metal-radical direct exchange coupling and SMM or single chain magnet (SCM) behavior, depending on the dimensionality.[13] Furthermore, recent studies revealed that NIT radicals containing aromatic -R groups can exhibit interesting electrical conductivity properties due to the presence of intermolecular π stacking between the NIT moiety and the aromatic ring of the phenyl substituent.[14]

With these thoughts in mind, we investigated the self-assembly reactions between Mn^{II} metal ions and NIT-PhOPh radical. NIT-PhOPh radical has been successfully employed in lanthanide chemistry to afford monomeric and polymeric species with fascinating magnetic properties.[15] However, the use of NIT-PhOPh radical with transition metal ions is very limited. Herein, we

report the high-yield synthesis, structure, and magnetic properties of a new manganese complex $[Mn^{II}(hfac)_2(IMHPhOPh)]_2[Mn^{II}(hfac)_3](IMH_2PhOPh)$ (**1**), containing both the reduced, IMHPhOPh, and the reduced protonated, IMH_2PhOPh, form of the NIT-PhOPh radical. The crystal structure of **1** is composed of three components, a mono- and a bi-metallic manganese complexes and an organic molecule, and it is stabilized via intermolecular interactions between the different moieties. Thus, **1** represents a rare example of a three-component co-crystal while it is a promising candidate for electronic conduction studies since the presence of many non-covalent interactions could favour the formation of intermolecular electron channels.

2. Experimental

2.1. Syntheses

All manipulations were performed under aerobic conditions using materials (reagent grade) and solvents as received. The starting materials NIT-PhOPh[10b] and $Mn(hfac)_2{\cdot}2H_2O$[16] were prepared according to literature procedures.

2.1.1. $[Mn^{II}(hfac)_2(IMHPhOPh)]_2[Mn^{II}(hfac)_3](IMH_2PhOPh)$ (1). To a stirred, boiling solution of dry n-heptane (50 mL) was added solid $Mn(hfac)_2{\cdot}2H_2O$ (0.05 g, 0.1 mmol). The resulting pale yellow solution was stirred for a further 20 min at 120°C, after which time it was cooled down to 75°C, and solid NITPhOPh radical (0.03 g, 0.1 mmol) was slowly added. CH_2Cl_2 (3 mL) was added and the dark blue solution was left to stand undisturbed. Slow evaporation of the solvent gave dark green crystals of **1** after a day which were collected by filtration and dried in air. The yield was 70%. Selected ATR data (cm^{-1}): 1645 (m), 1617 (w), 1590 (w), 1553 (w), 1526 (m), 1505 (m), 1488 (m), 1402 (w), 1380 (w), 1344 (w), 1306 (w), 1246 (s), 1195 (s), 1136 (s), 1026 (w), 1007 (w), 949 (w), 911 (w), 894 (w), 876 (w), 856 (w), 839 (w), 793 (m), 770 (w), 752 (w),

742 (w), 727 (w), 695 (w), 662 (s), 583 (m), 551 (w), 526 (w), 489 (w), 459 (w).

2.2. Single crystal X-ray crystallography

Table 1. Crystallographic data for complex **1**.

Compound	**1**
Formula	$C_{126}H_{100}F_{60}Mn_4N_8O_{28}$
$D_{calc.}$/ g cm^{-3}	1.626
μ / mm^{-1}	0.492
Formula Weight	3533.89
Colour	green
Shape	plate
Size/mm^3	0.070×0.040×0.015
T/K	100(2)
Crystal System	triclinic
Space Group	P-1
a/Å	10.9819(2)
b/Å	13.1391(3)
c/Å	25.4038(6)
α /°	96.833(2)
β /°	90.714(2)
γ /°	97.164(2)
V/Å^3	3609.74(14)
Z	1
Z'	0.5
Wavelength/Å	0.71075
Radiation type	Mo K_α
Θ_{min}/°	2.057
Θ_{max}/°	27.486
Measured Refl's.	56412
Indep't Refl's	16187
Refl's I≥2 σ(I)	10822
R_{int}	0.0794
Parameters	1146
Restraints	584
Largest Peak	0.709
Deepest Hole	-0.540
GooF	1.023
wR_2 (all data)	0.1172
wR_2	0.1044
R_1 (all data)	0.0892
R_1	0.0485

A green plate-shaped crystal of **1** with dimensions 0.070 × 0.040 × 0.015 mm^3 was mounted on a MITIGEN holder in perfluoroether oil. Data were collected using a Rigaku FRE+ equipped

with VHF Varimax confocal mirrors and an AFC12 goniometer and HyPix 6000 detector diffractometer equipped with an Oxford Cryosystems low-temperature device operating at T = 100(2) K. Data were measured using profile data from ω -scans of 0.5 ° per frame for 40.0 s using Mo K_α radiation (Rotating Anode, 45.0 kV, 55.0 mA). The diffraction pattern was indexed and the total number of runs and images was based on the strategy calculation from the program CrysAlisPro (Rigaku, V1.171.40.79a, 2020). The maximum resolution that was achieved was Θ = 27.486° (0.77 Å). The diffraction pattern was indexed and the total number of runs and images was based on the strategy calculation from the program CrysAlisPro (Rigaku, V1.171.40.79a, 2020). The unit cell was refined using CrysAlisPro (Rigaku, V1.171.40.79a, 2020) on 14382 reflections, 25% of the observed reflections. Data reduction, scaling and absorption corrections were performed using CrysAlisPro (Rigaku, V1.171.40.79a, 2020). The final completeness is 98.70 % out to 27.486° in Θ. A multi-scan absorption correction was performed using CrysAlisPro 1.171.40.79a (Rigaku Oxford Diffraction, 2020) Empirical absorption correction using spherical harmonics, implemented in SCALE3 ABSPACK scaling algorithm. The absorption coefficient μ of this material is 0.492 mm^{-1} at this wavelength (λ = 0.71075Å) and the minimum and maximum transmissions are 0.557 and 1.000. The structure was solved, and the space group P-1 (# 2) determined by the ShelXT 2018/2[17] structure solution program using using dual methods and refined by full matrix least squares minimisation on F^2 using version 2018/3 of ShelXL 2018/3[17]. All non-hydrogen atoms were refined anisotropically. Most hydrogen atom positions were calculated geometrically and refined using the riding model, but some hydrogen atoms were refined freely. There is disorder of several CF_3 groups. As such various geometrical (SADI) and displacement (SIMU, RIGU) restraints were employed. The value of Z' is 0.5. This means that

only half of the formula unit is present in the asymmetric unit, with the other half consisting of symmetry equivalent atoms.

2.3. Spectroscopic Measurements

Infrared spectra were obtained using a PerkinElmer Spectrum Two FT-IR Spectrometer.

EPR measurements were performed with a XXX ADD EPR Details HERE

2.4. Magnetic Measurements

Variable-temperature direct current (dc) magnetic susceptibility data were collected on a Quantum Design MPMS-XL SQUID magnetometer equipped with a 7 T magnet and operating in the 2-300 K range. The diamagnetic contribution of the sample holder was subtracted from the raw data. Pascal's constants[18] were used to estimate the diamagnetic corrections, which were subtracted from the experimental susceptibilities to give the molar paramagnetic susceptibilities (χ_M).

2.5. Electronic Conduction Measurements

The electrical conductivity of the system was measured with a home-made setup consisting of a two-point probe tester capable of detecting ultra-high-resistance . ADD DC CONDUCTIVITY Details HERE

3. Results and discussion

3.1. Synthesis

The reaction scheme $Mn(hfac)_2$/NIT-PhOPh was studied. High spin Mn(II) ions, due to their relatively isotropic ground state, are excellent candidates for probing the magnetic anisotropy of

specific coordination geometries in monometallic complexes [19] while they allow the development of magneto structural correlations in polynuclear compounds. [20] In the case of higher dimensionality species, Mn(II) compounds have provided model examples of one-dimensional Heisenberg magnets, especially when Mn(II) ions are bridged by NIT radicals.[21] Indeed, the general reaction scheme Mn(II)/NIT-R has been very flexible and several structures of various dimensionalities, depending on the -R substituent, have been reported. [11d, 21-22] Herein, we used the NIT-PhOPh radical since previous work[15] with rare earth ions has shown that this radical possesses two electron rich phenyl rings, that are separated by an ether group, which can be involved in stacking interactions with the hfac ligands, favouring the formation of 1D chains and providing interesting supramolecular features. The main weakness of this ligand, as for all NIT radicals, is the poor Lewis basicity which limits the coordination affinity to metal ions. To that end, $Mn(hfac)_2$ starting material, containing the electron withdrawing hexafluoroacetylacetonate (hfac) ancillary group, has been employed in order to enhance the binding of the NITPhOPh radical. In addition, the hfac groups occupies four coordination cities of the Mn(II) ions, leaving only two positions available for complexation with the radical, and thus, do not allow an increase in dimensionality beyond 0D complexes or 1D chain-like compounds.

To that end, the stoichiometric reaction (1:1) of $Mn(hfac)_2 \cdot 2H_2O$ and NITPhOPh in boiling n-heptane produced dark green crystals of $[Mn^{II}(hfac)_2(IMHPhOPh)]_2[Mn^{II}(hfac)_3](IMH_2PhOPh)$ (**1**),where IMHPhOPh is the three electron reduced form of the NITPhOPh nitronyl-nitroxide starting material, and IMH_2PhOPh is the protonated form of IMHPhOPh ligand, in 70% yield. The chemical and structural identity of the compound was confirmed by single-crystal X-ray crystallography and IR spectral data. The formula of **1** is based on metric parameters, charge-balance considerations, and bond valence sum (BVS) calculations on the Mn atoms.

The ligand IMHPhOPh was not initially added to the reaction but it was generated *in situ* from the NITPhOPh nitronyl nitroxide starting material in the presence of Mn^{II} ions. The conversion of NITPhOPh nitronyl nitroxide radical to the diamagnetic IMHPhOPh ligand includes a reduction of the nitronyl nitroxide radical to imino nitroxide radical (IMPhOPh) followed by another reduction of the latter to the diamagnetic IMHPhOPh moiety, which can exist in either the hydroxylamino or the amine-N-oxide form (Scheme 1). In this structure, the amine-N-oxide form of the IMHPhOPh ligand is favored since its oxygen atom is bridging the two metal ions. Similar transformations have been observed for other nitronyl nitroxide radicals and it is now well established that manganese ions in low oxidation states are essential for the reduction of nitronyl nitroxide radicals, however the mechanism of such reactions is still not clear.[23] Further evidence for the absence of the radical character of the IMHPhOPh ligand is provided by the N-O bond distance, 1.370(2) Å, which is significantly longer that the corresponding distance found in free or coordinated nitronyl nitroxides, ranging from 1.25 to 1.32 Å, and consistent with reports for analogous reduced radicals.[23]

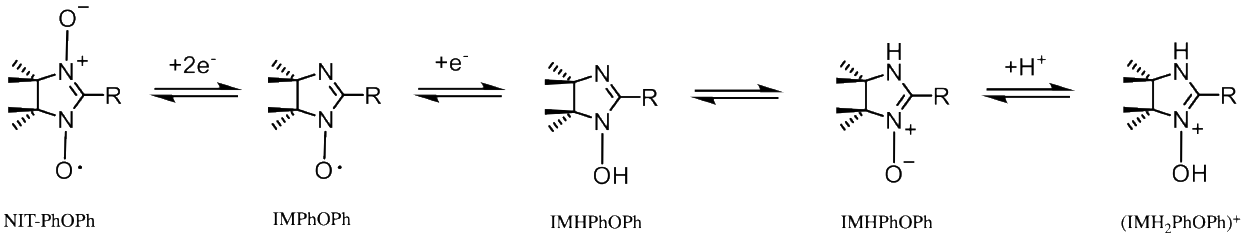

Scheme 1. Redox process of the NIT-PhOPh radical.

3.2. Description of the Structure

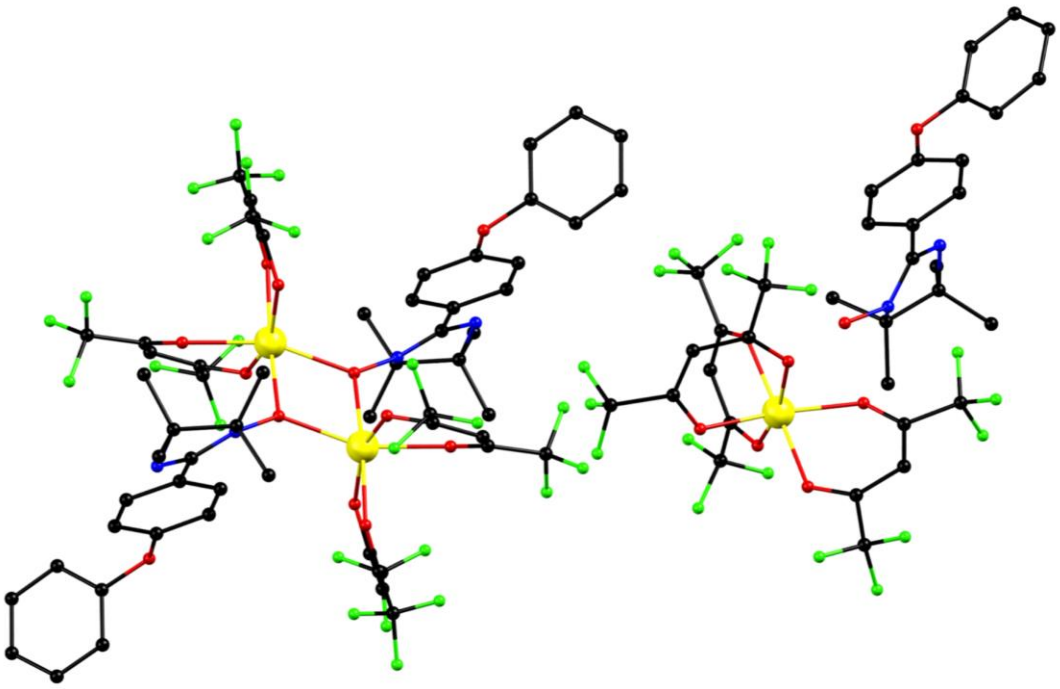

Figure 1. Crystal structure of **1**, showing the simultaneous presence of the monomer and dimer systems. H atoms were omitted for the sake of clarity. Color scheme: Mn, yellow; O, red; N, blue; F, green; C, black.

Complex **1** crystallizes in the triclinic space group $P\bar{1}$. A labeled representation of **1** is presented in Fig. 1. The asymmetric unit features one half of the bimetallic $[Mn(hfac)_2(IMHPhOPh)]_2$ complex, with the remainder related through an inversion center. The bimetallic complex in **1** crystallizes with a $[Mn^{II}(hfac)_3]^-$ anion and a $(IMH_2PhOPh)^+$ cation (Fig. S2). This is an interesting supramolecular feature of **1** since crystals containing more than two components are rare and have been observed mainly in organic systems. Formation of multicomponent crystals or co-crystals[24] has gained significant attention over the past years due the fact that the co-crystallized materials can improve the physicochemical properties of the single molecular components without altering their chemical integrity[25] . In general, crystal engineering principles [26] are employed for the

formation of a co-crystal consisting of an active compound and a selected co-crystal precursor which will transfer the desired property to the new system.[27] This strategy has been successful in the case of organic molecules and there are several reports demonstrating that co-crystallization of two different organic molecules is affecting the pharmaceutical,[28] magnetic,[29] optical,[30] or, mechanical[31] properties of the new structure. However, incorporation of metal coordination compounds into co-crystals is often challenging since metal complexes usually possess a variety of coordination modes and thus different crystallization kinetics and lattice packing forces. [32] Compound **1** constitutes a rare example of a three-component co-crystal in which two different metal complexes, a monometallic and a bimetallic one, are crystallized together with an organic molecule and interact exclusively through non-covalent interactions. Charge considerations require a formal Mn^{II} description for both the bimetallic and the monometallic units in **2** which is further supported by the Mn-O bond distances (all >2.132(2) Å) which clearly indicate the presence of Mn^{II} ions in both units. The assignment of the Mn oxidation state is confirmed by BVS[33] calculations (Table 2).

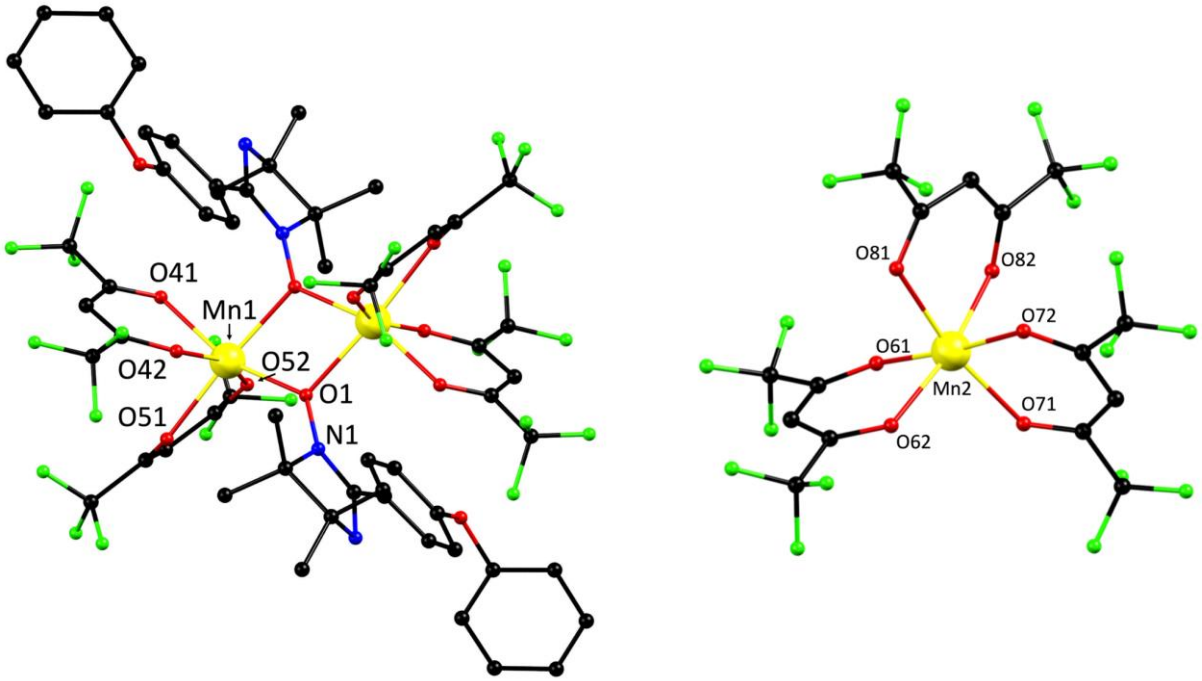

Figure 2. Labeled representation of the bimetallic $[Mn(hfac)_2(IMHPhOPh)]_2$ complex (left) and the $[Mn^{II}(hfac)_3]^-$ anion of **1**. H atoms were omitted for the sake of clarity. Color scheme: Mn, yellow; O, red; N, blue; F, green; C, black.

Table 2. Bond valence sum (BVS)[a] calculations for Mn atoms in **1**.

Atom	Mn^{II}	Mn^{III}
Mn1	<u>2.00</u>	1.84
Mn2	<u>2.07</u>	1.91

[a]The underlined value is the one closest to the charge for which it was calculated. The oxidation state is the nearest whole number to the underlined value.

In the bimetallic complex, the two $Mn(hfac)_2$ units are doubly bridged by the O-donor atoms of the IMHPhOPh ligand. Each Mn atom is 6-coordinate, possessing a distorted octahedral geometry,

with four coordination sites being occupied by two chelating hfac groups and the remaining two positions being filled by the O atoms of two bridging IMHPhOPh ligands. The Mn-O distances are ranging from 2.123(2) to 2.204(2) Å, in agreement with those reported for other Mn^{II}-containing compounds.[34] A close inspection of the supramolecular interactions revealed that the bimetallic complex is organized in pseudo 1-D chains due to the presence of non-covalent intermolecular F…F interactions between the CF_3 groups of the hfac ligands with a distance of 2.639(2) Å. The intramolecular Mn···Mn separation is 3.532(2) Å, with the closest intermolecular Mn···Mn contact being 10.184(2) Å.

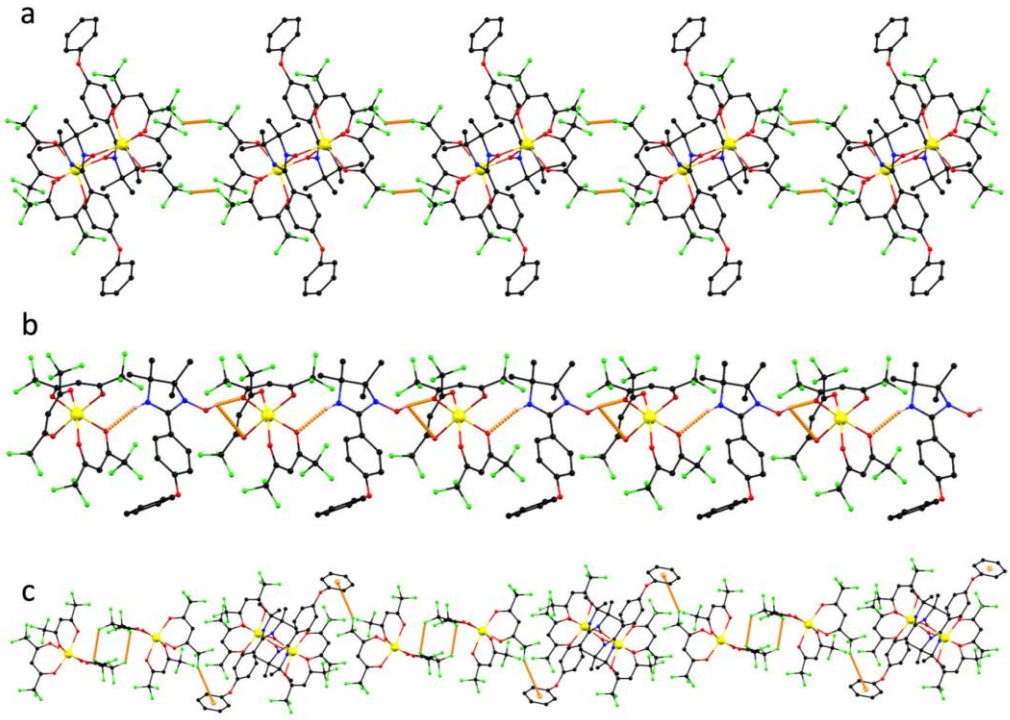

Figure 3. Intermolecular interactions in **1**. Color scheme: Mn, yellow; O, red; N, blue; F, green; C, black; H, salmon.

In the homoleptic $[Mn^{II}(hfac)_3]^-$ mononuclear moiety, the central Mn ion is in a distorted octahedral geometry and it is surrounded by the oxygen donor atoms of three chelating hfac ligands. The Mn-O bond distances in the anion of **1** are in the same range (average value 2.153(2) Å) with values previously reported for other complexes containing the $[Mn^{II}(hfac)_3]^-$ unit[34] and significantly longer that those found in neutral $[Mn^{III}(hfac)_3]$ species.[35] Another notable difference between the latter species and the anion of **1** is the lack of the Jahn-Teller distortion observed in **1**, which further supports the presence of Mn^{II} ion in the mononuclear moiety of **1**.[36] The oxygen atoms of the hfac groups of the $[Mn^{II}(hfac)_3]^-$ mononuclear moiety are involved in intermolecular hydrogen bonding interactions with the free $(IMH_2PhOPh)^+$ cations. Indeed, the $(IMH_2PhOPh)^+$ cation interacts with the O atoms of three different hfac groups through both the -NH and the -OH groups, involving the $(IMH_2PhOPh)^+$ O atom, O21, and the N atom, N22 as the donors, and the hfac O atoms, O62, O72, and O82 as the acceptors, with relatively short -NH…O and -OH…O hydrogen bonding distances (-NH…O 2.900(2) Å, -OH…O 2.670(2) Å, and -OH…O 2.818(2) Å) (Figure 3). In addition, a close inspection of the intermolecular contacts in **1** revealed the presence of non-covalent F…F interactions between the CF_3 groups of the hfac ligands of the $[Mn^{II}(hfac)_3]^-$ mononuclear moiety with a distance of 2.877(2) Å. The $[Mn^{II}(hfac)_3]^-$ is also connected intermolecularly with the bimetallic $[Mn(hfac)_2(IMHPhOPh)]_2$ complex through CF_3…π interactions between the hfac groups and the phenyl substituent of the coordinated IMHPhOPh ligand (3.650(2) Å). The closest intermolecular Mn1…Mn1 contact is 8.060(2) Å, with the Mn1…Mn2 separation being 10.740(2) Å.

3.3. Magnetic Studies

Variable temperature direct current (*dc*) magnetic susceptibility measurements were performed on powdered polycrystalline sample of **1** in a 0.1 T field and in the 2 - 300 K range. The $\chi_M T$ versus T plot is depicted in Fig. 4. For **1**, the experimental $\chi_M T$ value (12.9(2) emu K mol^{-1}) at 300 K is in good agreement with the expected one (13.1 emu K mol^{-1}) for three non-interacting Mn^{II} ions. Upon cooling, $\chi_M T$ slightly decreases till 100 K, below which temperature $\chi_M T$ decreases more rapidly, reaching a minimum value of 1.4(2) emu K mol^{-1} at 2 K. The overall magnetic response of **1** is suggestive of the presence of weak antiferromagnetic coupling between the Mn^{II} ions within the dimeric unit of **1**. In order to estimate the intramolecular magnetic exchange interactions between the metal ions of bimetallic complex the magnetic susceptibility data for **1** were fit using PHI[37] program, using the following spin Hamiltonian: $\hat{H} = -2J(S_{Mn_1}S_{Mn_1'})$.

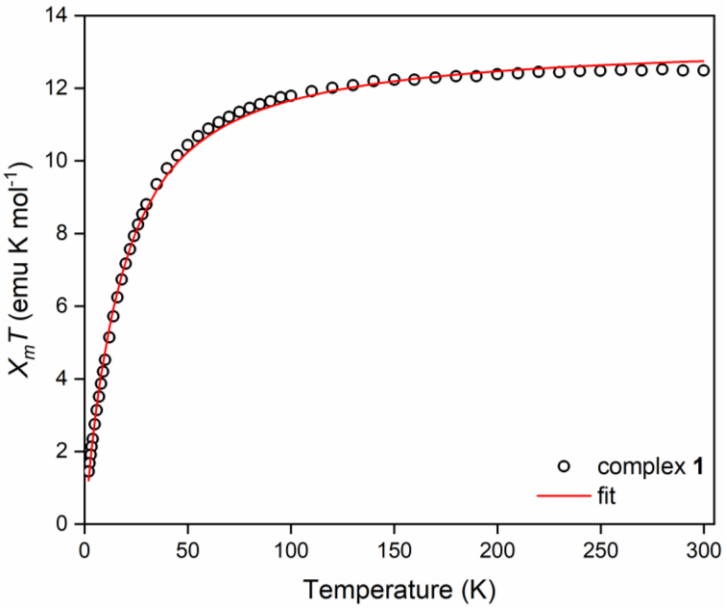

Figure 4. Temperature dependence of the $\chi_M T$ product for **1**, black solid line represents the fit of the data using PHI program (fitting parameters: J = -0.79(1) cm^{-1} and g = 2.04(1)).

The fit gave the following parameters: J = -0.79(1) cm^{-1} and g = 2.04(1). Inclusion of an intermolecular exchange constant of up to zJ = - 0.01 cm^{-1} did not improve the fitting and gave nearly identical J values. These results revealed the presence of weak antiferromagnetic interactions between the Mn^{II} ions in the dimeric unit of **1**. The obtained coupling constant is similar with values reported for Mn(II) complexes with the same topology containing other reduced imino nitroxide radicals (IMH-R) like the furfural (-0.86 cm^{-1})[23c] and the phenyl (-0.88 cm^{-1}) [23a, 23b] derivatives while it is lower than that observed for the reduced bithiophene (-1.55 cm^{-1})[23d] derivative. As expected, the value of Mn(II)-Mn(II) exchange in the dimeric unit of **1** is considerable lower that those reported for the Mn(II)-radical exchange in similar systems using nitronyl nitroxide (-50 cm^{-1} and -71 cm^{-1} for the 4-fluorophenyl[38] and methyl[39] analogues, respectively) or imino nitroxide (-9.36 cm^{-1} for 4-chlorophenyl[23e]) radicals.

3.4. Electron Paramagnetic Resonance

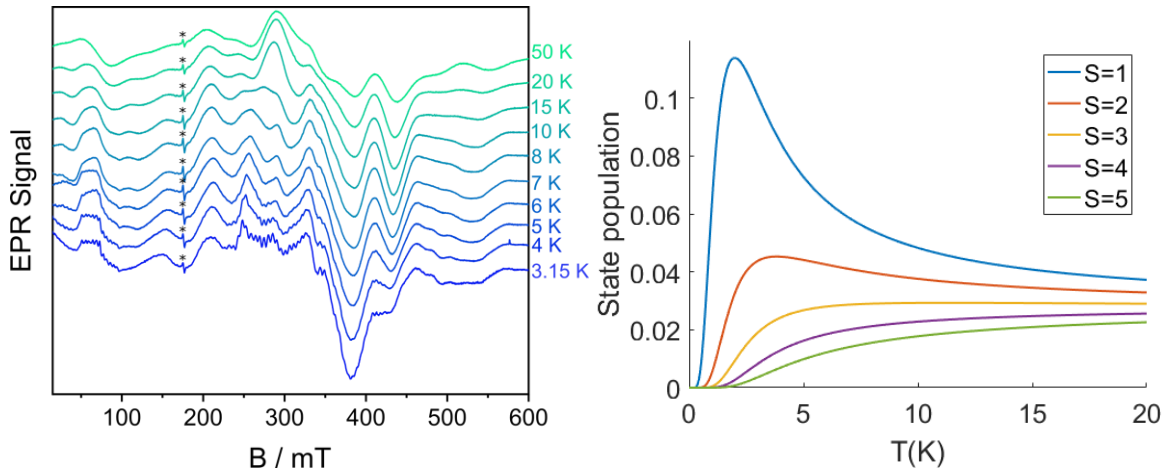

Figure 5. ADD CAPTION HERE

EPR spectroscopy has been a powerful technique for elucidating the magnetic properties of manganese containing compounds. [19b, 40] High-spin mononuclear Mn(II) complexes have a ground state of S = 5/2 while zero-field-splitting (ZFS) lifts the degeneracy of the ground state, generating three Kramer's doublets |±1/2〉, |±3/2〉 and, |±5/2〉. [40n] As a result, EPR spectra of mononuclear Mn(II) complexes usually consist of a six-line signal concentrated at around g = 2, which is temperature dependent (signal's intensity is decreasing on increasing temperature). On the other hand, bimetallic Mn(II) compounds possess an effective spin ground of S = 5 which can be split to electron-spin energy levels associated with integer spin values ranging from 0 to 5. Bimetallic Mn(II) compounds show a characteristic 11-line hyperfine pattern in EPR spectra, which is broad and strongly temperature dependent.[40l] Analysis of their EPR spectra offers the opportunity to determine important parameters, including the strength of the exchange coupling, the dipolar coupling, the isotropic g-factor and, the D and E zero-field splitting parameters. Thus, EPR experiments were performed on polycrystalline powder samples of 1 at temperatures of 3.15-50 K in order to gain information about the dipolar coupling between the metal ions and the zero field splitting parameters in **1**.

The spectra in Figure 5 show the EPR signal of a polycrystalline powder of **1** at different temperatures. The spectra can be interpreted as a superposition of signals from a Mn monomer and an independent Mn dimer. The Mn monomer has S = 5/2, while the dimer can be treated as an effective spin S = 5 according to the theory developed in (Bencini, Gatteschi, 1992). The antiferromagnetic $2J$ coupling in the dimer (-1.58 cm^{-1} as measured by SQUID) is larger than the frequency of the measurements (0.324 cm^{-1}), hence placing the system in a regime where the microwaves cannot drive transition between states of different S. Due to the large number of simultaneous contributions, we were unable to extract the parameters of the monomer and the

dimer, but we can offer a qualitative explanation. States with different *S* get populated increasing the temperature and their contribution is matched in the spectra. At 3.15 K the contribution from the dimer comes from the *S* = 1, *S* = 2, and *S* = 3 states. Particularly, the 11 lines at 60 mT are a signature of the $\Delta m_s = \pm 2$ transition of the *S* = 1 state mixed with the isotropic hyperfine coupling of two Mn nuclei. The intensity of this transition quickly decreases when increasing the temperature, because the *S* = 1 state gets depopulated in favor of higher spin states. Similarly, the hyperfine lines between 250 and 350 mT that are related to the *S* = 2 level, also decrease in intensity when the state is depopulated. On the other hand, the peaks at 280 and 440 mT increase in intensity since they represent the contribution of *S* = 4 and *S* = 5.

3.5. Electrical Conductivity

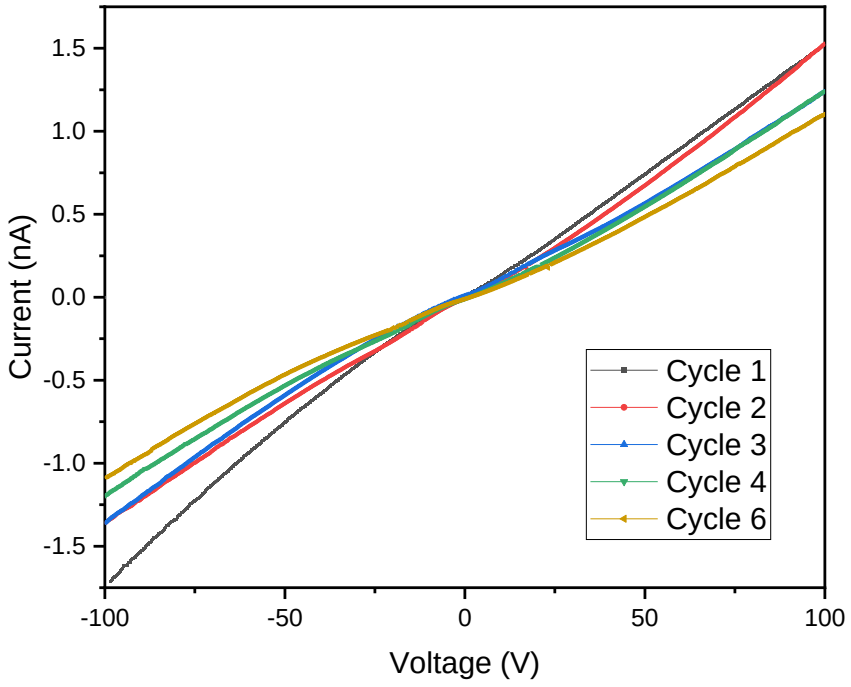

Figure 6. Current-Voltage characteristic of **1** showing six repeated cycles. The voltage sweeping rate is 0.2 V/s.

Recently, molecular magnetic materials have been proposed for applications in the area of spintronics where the magnetic properties can be used to tune the transport properties of electronic devices.[41] A central challenge in the design of such materials is the presence of intra- and inter-molecular electronic channels which can be tuned by using rational chemical design. Compound **1** is a promising candidate for electronic conduction studies since the presence of many non-covalent interactions between the three different components is indicative of the presence of possible intermolecular electron channels. In addition, we have shown, previously, that NIT-R radicals containing aromatic -R substituents, like the NIT-PhOPh radical used here, do not exhibit the typical Mott insulator behaviour but they possess electron transport channels due to the intermolecular π stacking between the aromatic ring of the phenyl substituent and the delocalized NIT moiety.[14] To that end experiments were performed in order to investigate the transport characteristics of **1**.

Figure 6 shows an example of the I-V curve for a single crystal of **1**. A low sweeping rate was used for all the measurements to minimize the hysteresis effect. The curves are almost straight lines, indicating that the electrical conduction is dominated by Ohm's law in **1**. Considering the crystal structure, the charge carriers in a single crystal of **1** should be mostly localized, and the transport includes both intramolecular and intermolecular hopping.[42] Space Charge Limited Transport (SCLT)[43] was initial expected, because intermolecular hopping usually comes with large energy barrier, and results in very low carrier mobility.[14] However, SCLT was not observed in **1**, possibly due to the presence of strong intermolecular interactions, for instance the F…F, CF_3…π interactions and hydrogen bonding. The slight degradation of the conductance that observed over repeated sweeping cycles (Figure 6) can be mainly attributed to the damaged contact interface under prolonged bias voltage stress. Therefore, we tried to eliminate the measuring time for each

crystal by performing short experiments. Finally, we averaged the slopes from totally 24 sweeping curves, and then calculate the conductance value, which is $1.34(62) \times 10^{-9}$ S/cm.

4. Conclusions

In summary, a new manganese (II) dimer, $[Mn(hfac)_2(IMHPhOPh)]_2$, bridged by the oxygen atoms of the diamagnetic IMHPhOPh ligand, which derived from the reduction of the NIT-PhOPh radical. Interestingly, the bimetallic complex crystallizes with a $[Mn^{II}(hfac)_3]^-$ anion and a $(IMH_2PhOPh)^+$ cation. A close inspection of the crystal structure of **1** revealed the presence of non-covalent intermolecular interactions between all three species. Complex **1** exhibits an overall antiferromagnetic behavior while fitting of the experimental data revealed a coupling constant of J = -0.79(1) cm^{-1} for the Mn^{II} dinmer. Work in progress includes the extension of this work using other nitronyl-nitroxide radicals, with various substituents, in order to gain access to radical-bridged manganese compounds.

Acknowledgements

We acknowledge funding from the European Union (ERC-CoG-773048-MMGNRs), the Royal Society (University Research Fellow and URF grant), UK-EPSRC EP/L011972/1, and XXX.

The X-ray diffractometer and SQUID magnetometer used in this research were

Appendix A. Supplementary data

CCDC 1828436 contains the supplementary crystallographic data for complex **1**.

References:

1. aR. Sessoli, D. Gatteschi, A. Caneschi and M. A. Novak, *Nature*, 1993, **365**, 141-143; bR. Sessoli, H. L. Tsai, A. R. Schake, S. Wang, J. B. Vincent, K. Folting, D. Gatteschi, G. Christou and D. N. Hendrickson, *Journal of the American Chemical Society*, 1993, **115**, 1804-1816; cG. Christou, D. Gatteschi, D. N. Hendrickson and R. Sessoli, *MRS Bulletin*, 2000, **25**, 66-71; dD. Gatteschi and R. Sessoli, *Angewandte Chemie International Edition*, 2003, **42**, 268-297; eA. J. Tasiopoulos, A. Vinslava, W. Wernsdorfer, K. A. Abboud and G. Christou, *Angewandte Chemie International Edition*, 2004, **43**, 2117-2121; fC. J. Milios, A. Vinslava, W. Wernsdorfer, S. Moggach, S. Parsons, S. P. Perlepes, G. Christou and E. K. Brechin, *Journal of the American Chemical Society*, 2007, **129**, 2754-2755; gR. Bagai and G. Christou, *Chemical Society Reviews*, 2009, **38**, 1011-1026.
2. aG. Christou, *Accounts of Chemical Research*, 1989, **22**, 328-335; bS. Mukhopadhyay, S. K. Mandal, S. Bhaduri and W. H. Armstrong, *Chemical Reviews*, 2004, **104**, 3981-4026; cJ. Raymond and R. E. Blankenship, *Coordination Chemistry Reviews*, 2008, **252**, 377-383; dJ. G. McAlpin, T. A. Stich, W. H. Casey and R. D. Britt, *Coordination Chemistry Reviews*, 2012, **256**, 2445-2452; eM. D. Kärkäs, O. Verho, E. V. Johnston and B. Åkermark, *Chemical Reviews*, 2014, **114**, 11863-12001; fF. Yu, V. M. Cangelosi, M. L. Zastrow, M. Tegoni, J. S. Plegaria, A. G. Tebo, C. S. Mocny, L. Ruckthong, H. Qayyum and V. L. Pecoraro, *Chemical Reviews*, 2014, **114**, 3495-3578; gK. J. Young, B. J. Brennan, R. Tagore and G. W. Brudvig, *Accounts of Chemical Research*, 2015, **48**, 567-574; hB. Gerey, E. Gouré, J. Fortage, J. Pécaut and M.-N. Collomb, *Coordination Chemistry Reviews*, 2016, **319**, 1-24; iM. M. Najafpour, I. Zaharieva, Z. Zand, S. Maedeh Hosseini, M. Kouzmanova, M. Hołyńska, I. Tranca, A. W. Larkum, J.-R. Shen and S. I. Allakhverdiev, *Coordination Chemistry Reviews*, 2020, **409**, 213183; jA. J. Wu, J. E. Penner-Hahn and V. L. Pecoraro, *Chemical Reviews*, 2004, **104**, 903-938; kS. Signorella and C. Hureau, *Coordination Chemistry Reviews*, 2012, **256**, 1229-1245; lA. J. L. Villaraza, A. Bumb and M. W. Brechbiel, *Chemical Reviews*, 2010, **110**, 2921-2959.
3. R. D. Dowsing and J. F. Gibson, *The Journal of Chemical Physics*, 1969, **50**, 294-303.
4. aG. H. Reed and M. Cohn, *Journal of Biological Chemistry*, 1970, **245**, 662-664; bG. H. Reed and G. D. Markham, in *Biological Magnetic Resonance: Volume 6*, eds. L. J. Berliner and J. Reuben, Springer US, Boston, MA, 1984, DOI: 10.1007/978-1-4615-6546-8_3, pp. 73-142; cW. R. Hagen, *Coordination Chemistry Reviews*, 1999, **190-192**, 209-229; dJ. Krzystek, A. Ozarowski and J. Telser, *Coordination Chemistry Reviews*, 2006, **250**, 2308-2324; eT. A. Stich, S. Lahiri, G. Yeagle, M. Dicus, M. Brynda, A. Gunn, C. Aznar, V. J. Derose and R. D. Britt, *Appl Magn Reson*, 2007, **31**, 321-341; fA. I. Poddel'sky, V. K. Cherkasov and G. A. Abakumov, *Coordination Chemistry Reviews*, 2009, **253**, 291-324; gD. M. Gagnon, R. C. Hadley, A. Ozarowski, E. M. Nolan and R. D. Britt, *The Journal of Physical Chemistry B*, 2019, **123**, 4929-4934.
5. D. Gatteschi, A. L. Barra, A. Caneschi, A. Cornia, R. Sessoli and L. Sorace, *Coordination Chemistry Reviews*, 2006, **250**, 1514-1529.
6. R. Vincent, S. Klyatskaya, M. Ruben, W. Wernsdorfer and F. Balestro, *Nature*, 2012, **488**, 357.
7. aL. Bogani and W. Wernsdorfer, *Nature Materials*, 2008, **7**, 179; bM. Urdampilleta, S. Klyatskaya, J. P. Cleuziou, M. Ruben and W. Wernsdorfer, *Nat. Mater.*, 2011, **10**, 502.
8. aG. Aromí and E. K. Brechin, in *Single-Molecule Magnets and Related Phenomena*, ed. R. Winpenny, Springer Berlin Heidelberg, Berlin, Heidelberg, 2006, DOI: 10.1007/430_022, pp. 1-67; bJ. R. Friedman and M. P. Sarachik, *Annu. Rev. Condens. Matter Phys.*, 2010, **1**,

109-128; cC. J. Milios and R. E. P. Winpenny, in *Molecular Nanomagnets and Related Phenomena*, ed. S. Gao, Springer Berlin Heidelberg, Berlin, Heidelberg, 2015, DOI: 10.1007/430_2014_149, pp. 1-109.
9. S. Demir, I.-R. Jeon, J. R. Long and T. D. Harris, *Coordination Chemistry Reviews*, 2015, **289-290**, 149-176.
10. aA. Caneschi, D. Gatteschi and P. Rey, *Progress in Inorganic Chemistry*, 1991, DOI: doi:10.1002/9780470166406.ch6
10.1002/9780470166406.ch6, 331-429; bE. F. Ullman, J. H. Osiecki, D. G. B. Boocock and R. Darcy, *Journal of the American Chemical Society*, 1972, **94**, 7049-7059.
11. aC. Benelli and D. Gatteschi, *Chemical Reviews*, 2002, **102**, 2369-2388; bL. Bogani, *Journal of Applied Physics*, 2011, **109**, 07B115; cX. Meng, W. Shi and P. Cheng, *Coordination Chemistry Reviews*, 2019, **378**, 134-150; dD. Luneau, *European Journal of Inorganic Chemistry*, 2020, **2020**, 597-604.
12. aM. Zhu, Y.-G. Li, Y. Ma, L.-C. Li and D.-Z. Liao, *Inorganic Chemistry*, 2013, **52**, 12326-12328; bM. Zhu, P. Hu, Y. Li, X. Wang, L. Li, D. Liao, V. M. L. Durga Prasad Goli, S. Ramasesha and J.-P. Sutter, *Chemistry – A European Journal*, 2014, **20**, 13356-13365; cJ. Wang, M. Zhu, C. Li, J. Zhang and L. Li, *European Journal of Inorganic Chemistry*, 2015, **2015**, 1368-1375; dX.-F. Wang, P. Hu, Y.-G. Li and L.-C. Li, *Chemistry – An Asian Journal*, 2015, **10**, 325-328; eM. Zhu, M. Yang, J. Wang, H. Li and L. Li, *Chemistry – An Asian Journal*, 2016, **11**, 1900-1905; fA. A. Patrascu, S. Calancea, M. Briganti, S. Soriano, A. M. Madalan, R. A. A. Cassaro, A. Caneschi, F. Totti, M. G. F. Vaz and M. Andruh, *Chemical Communications*, 2017, **53**, 6504-6507; gB. Yao, Z. Guo, X. Zhang, Y. Ma, Z. Yang, Q. Wang, L. Li and P. Cheng, *Crystal Growth & Design*, 2017, **17**, 95-99; hX. Liu, Y. Zhang, W. Shi and P. Cheng, *Inorganic Chemistry*, 2018, **57**, 13409-13414; iH. Li, J. Sun, M. Yang, Z. Sun, J. Tang, Y. Ma and L. Li, *Inorganic Chemistry*, 2018, **57**, 9757-9765; jJ. Xie, H.-D. Li, M. Yang, J. Sun, L.-C. Li and J.-P. Sutter, *Chemical Communications*, 2019, **55**, 3398-3401; kL. Xi, H. Li, J. Sun, Y. Ma, J. Tang and L. Li, *Inorganic Chemistry*, 2020, **59**, 443-451; lL. Xi, J. Sun, K. Wang, J. Lu, P. Jing and L. Li, *Dalton Transactions*, 2020, **49**, 1089-1096.
13. aC. Benelli, A. Caneschi, D. Gatteschi, L. Pardi and P. Rey, *Inorganic Chemistry*, 1989, **28**, 275-280; bC. Benelli, A. Caneschi, D. Gatteschi and R. Sessoli, *Advanced Materials*, 1992, **4**, 504-505; cC. Benelli, A. Caneschi, D. Gatteschi and R. Sessoli, *Inorganic Chemistry*, 1993, **32**, 4797-4801.
14. N. Dotti, E. Heintze, M. Slota, R. Hübner, F. Wang, J. Nuss, M. Dressel and L. Bogani, *Physical Review B*, 2016, **93**, 165201.
15. aL. Bogani, C. Sangregorio, R. Sessoli and D. Gatteschi, *Angewandte Chemie International Edition*, 2005, **44**, 5817-5821; bK. Bernot, L. Bogani, A. Caneschi, D. Gatteschi and R. Sessoli, *Journal of the American Chemical Society*, 2006, **128**, 7947-7956.
16. F. A. Cotton and R. H. Holm, *Journal of the American Chemical Society*, 1960, **82**, 2979-2983.
17. G. M. Sheldrick, *Acta Crystallogr. Sect. A, Found. and Adv.*, 2015, **71**, 3-8.
18. G. A. Bain and J. F. Berry, *J. Chem. Educ.*, 2008, **85**, 532.
19. aM. A. Hay, A. Sarkar, K. E. R. Marriott, C. Wilson, G. Rajaraman and M. Murrie, *Dalton Transactions*, 2019, **48**, 15480-15486; bS. Zein, C. Duboc, W. Lubitz and F. Neese, *Inorganic Chemistry*, 2008, **47**, 134-142.

20. aT. K. Karmakar, B. K. Ghosh, A. Usman, H.-K. Fun, E. Rivière, T. Mallah, G. Aromí and S. K. Chandra, *Inorganic Chemistry*, 2005, **44**, 2391-2399; bK. R. Vignesh, S. K. Langley, C. J. Gartshore, B. Moubaraki, K. S. Murray and G. Rajaraman, *Inorganic Chemistry*, 2017, **56**, 1932-1949.
21. A. Caneschi, D. Gatteschi, N. Lalioti, C. Sangregorio and R. Sessoli, *Journal of the Chemical Society, Dalton Transactions*, 2000, DOI: 10.1039/B004244G, 3907-3912.
22. aM. Fettouhi, M. Khaled, A. Waheed, S. Golhen, L. Ouahab, J.-P. Sutter and O. Kahn, *Inorganic Chemistry*, 1999, **38**, 3967-3971; bD. Luneau, A. Borta, Y. Chumakov, J.-F. Jacquot, E. Jeanneau, C. Lescop and P. Rey, *Inorganica Chimica Acta*, 2008, **361**, 3669-3676.
23. aA. Caneschi, D. Gatteschi, J. Laugier, P. Rey and C. Zanchini, *Inorganic Chemistry*, 1989, **28**, 1969-1975; bM. D. Carducci and R. J. Doedens, *Inorganic Chemistry*, 1989, **28**, 2492-2494; cZ.-H. Jiang, B.-W. Sun, D.-Z. Liao, G.-L. Wang, B. Donnadieu and J.-P. Tuchagues, *Inorganica Chimica Acta*, 1998, **279**, 76-84; dL.-Y. Wang, X.-Q. Wang, K. Jiang, J.-L. Chang and Y.-F. Wang, *Journal of Molecular Structure*, 2007, **840**, 14-21; eX.-H. Lv, S.-L. Yang, Y.-X. Li, C.-X. Zhang and Q.-L. Wang, *Journal of Molecular Structure*, 2017, **1133**, 211-216.
24. aG. R. Desiraju, *CrystEngComm*, 2003, **5**, 466-467; bJ. D. Dunitz, *CrystEngComm*, 2003, **5**, 506-506; cA. D. Bond, *CrystEngComm*, 2007, **9**, 833-834.
25. aA. O. Surov, K. A. Solanko, A. D. Bond, G. L. Perlovich and A. Bauer-Brandl, *Crystal Growth & Design*, 2012, **12**, 4022-4030; bM. Joshi and A. Roy Choudhury, *ACS Omega*, 2018, **3**, 2406-2416; cW. Dohle, A. E. Prota, G. Menchon, E. Hamel, M. O. Steinmetz and B. V. L. Potter, *ACS Omega*, 2019, **4**, 755-764; dX.-S. Gao, H.-J. Dai, Y. Tang, M.-J. Ding, W.-B. Pei and X.-M. Ren, *ACS Omega*, 2019, **4**, 12230-12237.
26. aG. R. Desiraju, *Journal of Molecular Structure*, 2003, **656**, 5-15; bG. R. Desiraju, *Journal of Chemical Sciences*, 2010, **122**, 667-675; cG. R. Desiraju, *Journal of the American Chemical Society*, 2013, **135**, 9952-9967; dG. Desiraju, *IUCrJ*, 2018, **5**, 660.
27. S. Aitipamula, P. S. Chow and R. B. H. Tan, *CrystEngComm*, 2014, **16**, 3451-3465.
28. Ö. Almarsson and M. J. Zaworotko, *Chemical Communications*, 2004, DOI: 10.1039/B402150A, 1889-1896.
29. H. Akpinar, J. T. Mague, M. A. Novak, J. R. Friedman and P. M. Lahti, *CrystEngComm*, 2012, **14**, 1515-1526.
30. aX. Fang, X. Yang and D. Yan, *Journal of Materials Chemistry C*, 2017, **5**, 1632-1637; bS. Li and D. Yan, *Advanced Optical Materials*, 2018, **6**, 1800445.
31. S. Karki, T. Friščić, L. Fábián, P. R. Laity, G. M. Day and W. Jones, *Advanced Materials*, 2009, **21**, 3905-3909.
32. aA. Biswas, M. Ghosh, P. Lemoine, S. Sarkar, S. Hazra and S. Mohanta, *European Journal of Inorganic Chemistry*, 2010, **2010**, 3125-3134; bH. Hadadzadeh, G. Mansouri, A. R. Rezvani and H. R. Khavasi, *Journal of Chemical Crystallography*, 2012, **42**, 486-493; cR. Golbedaghi, S. Salehzadeh, H. R. Khavasi and A. G. Blackman, *Polyhedron*, 2014, **68**, 151-156; dL. K. Das, A. Biswas, C. J. Gómez-García, M. G. B. Drew and A. Ghosh, *Inorganic Chemistry*, 2014, **53**, 434-445.
33. aW. Liu and H. H. Thorp, *Inorganic Chemistry*, 1993, **32**, 4102-4105; bI. D. Brown and D. Altermatt, *Acta Crystallographica Section B*, 1985, **41**, 244-247.
34. aS. Shibata, S. Onuma and H. Inoue, *Chemistry Letters*, 1984, **13**, 485-486; bS. Shibata, S. Onuma and H. Inoue, *Inorganic Chemistry*, 1985, **24**, 1723-1725; cF. A. Villamena, M. H.

Dickman and D. R. Crist, *Inorganic Chemistry*, 1998, **37**, 1446-1453; dG. Aromí, P. Carrero Berzal, P. Gamez, O. Roubeau, H. Kooijman, A. L. Spek, W. L. Driessen and J. Reedijk, *Angewandte Chemie International Edition*, 2001, **40**, 3444-3446; eJ. R. Bryant, J. E. Taves and J. M. Mayer, *Inorganic Chemistry*, 2002, **41**, 2769-2776; fH. Zhang, B. Li, J. Sun, R. Clérac and E. V. Dikarev, *Inorganic Chemistry*, 2008, **47**, 10046-10052; gH. Zhang, B. Li and E. V. Dikarev, *Journal of Cluster Science*, 2008, **19**, 311-321; hH. Zhang, J.-H. Yang, R. V. Shpanchenko, A. M. Abakumov, J. Hadermann, R. Clérac and E. V. Dikarev, *Inorganic Chemistry*, 2009, **48**, 8480-8488; iA. Navulla, L. Huynh, Z. Wei, A. S. Filatov and E. V. Dikarev, *Journal of the American Chemical Society*, 2012, **134**, 5762-5765; jZ. Wei, A. S. Filatov and E. V. Dikarev, *Journal of the American Chemical Society*, 2013, **135**, 12216-12219; kC. M. Lieberman, Z. Wei, A. S. Filatov and E. V. Dikarev, *Inorganic Chemistry*, 2016, **55**, 3946-3951; lM. C. Barry, C. M. Lieberman, Z. Wei, R. Clérac, A. S. Filatov and E. V. Dikarev, *Inorganic Chemistry*, 2018, **57**, 2308-2313; mM. Hakimi, M. Alikhani, M. Mashreghi, N. Feizi, H. Raeisi, Y. Mirzai, V. Eigner and M. Dusek, *Journal of Molecular Structure*, 2019, **1186**, 355-361.

35. E. Bouwman, K. G. Caulton, G. Christou, K. Folting, C. Gasser, D. N. Hendrickson, J. C. Huffman, E. B. Lobkovsky and J. D. Martin, *Inorganic Chemistry*, 1993, **32**, 3463-3470.
36. R. Freitag and J. Conradie, *Journal of Chemical Education*, 2013, **90**, 1692-1696.
37. I. A. Gass, S. Tewary, A. Nafady, N. F. Chilton, C. J. Gartshore, M. Asadi, D. W. Lupton, B. Moubaraki, A. M. Bond, J. F. Boas, S.-X. Guo, G. Rajaraman and K. S. Murray, *Inorganic Chemistry*, 2013, **52**, 7557-7572.
38. C.-X. Zhang, X.-Y. Zhao, N.-N. Sun, Y.-L. Guo and Y. Zhang, *Inorganica Chimica Acta*, 2011, **367**, 135-140.
39. C. Benelli, A. Caneschi, D. Gatteschi, M. C. Melandri and P. Rey, *Inorganica Chimica Acta*, 1990, **172**, 137-139.
40. aS. Blanchard, G. Blondin, E. Rivière, M. Nierlich and J.-J. Girerd, *Inorganic Chemistry*, 2003, **42**, 4568-4578; bD. Akhmetzyanov, J. Plackmeyer, B. Endeward, V. Denysenkov and T. F. Prisner, *Physical Chemistry Chemical Physics*, 2015, **17**, 6760-6766; cJ. Krzystek, J. Telser, J. Li and M. A. Subramanian, *Inorganic Chemistry*, 2015, **54**, 9040-9045; dC. Duboc, *Chemical Society Reviews*, 2016, **45**, 5834-5847; eM. Retegan, M.-N. Collomb, F. Neese and C. Duboc, *Physical Chemistry Chemical Physics*, 2013, **15**, 223-234; fC. Duboc, T. Phoeung, S. Zein, J. Pécaut, M.-N. Collomb and F. Neese, *Inorganic Chemistry*, 2007, **46**, 4905-4916; gC. Duboc, D. Ganyushin, K. Sivalingam, M.-N. Collomb and F. Neese, *The Journal of Physical Chemistry A*, 2010, **114**, 10750-10758; hC. Mantel, C. Baffert, I. Romero, A. Deronzier, J. Pécaut, M.-N. Collomb and C. Duboc, *Inorganic Chemistry*, 2004, **43**, 6455-6463; iC. Duboc, M.-N. Collomb and F. Neese, *Applied Magnetic Resonance*, 2009, **37**, 229; jM. Zlatar, M. Gruden, O. Y. Vassilyeva, E. A. Buvaylo, A. N. Ponomarev, S. A. Zvyagin, J. Wosnitza, J. Krzystek, P. Garcia-Fernandez and C. Duboc, *Inorganic Chemistry*, 2016, **55**, 1192-1201; kR. Gupta, T. Taguchi, A. S. Borovik and M. P. Hendrich, *Inorganic Chemistry*, 2013, **52**, 12568-12575; lS. Blanchard, G. Blain, E. Rivière, M. Nierlich and G. Blondin, *Chemistry – A European Journal*, 2003, **9**, 4260-4268; mA. P. Golombek and M. P. Hendrich, *Journal of Magnetic Resonance*, 2003, **165**, 33-48; nA. R. Coffino and J. Peisach, *Journal of Magnetic Resonance, Series B*, 1996, **111**, 127-134.
41. aA. R. Rocha, V. M. García-suárez, S. W. Bailey, C. J. Lambert, J. Ferrer and S. Sanvito, *Nature Materials*, 2005, **4**, 335-339; bL. Bogani and W. Wernsdorfer, *Nature Materials*,

2008, **7**, 179-186; cS. Sanvito, *Chemical Society Reviews*, 2011, **40**, 3336-3355; dR. Vincent, S. Klyatskaya, M. Ruben, W. Wernsdorfer and F. Balestro, *Nature*, 2012, **488**, 357-360.
42. L. S. Xie, G. Skorupskii and M. Dincă, *Chemical Reviews*, 2020, **120**, 8536-8580.
43. M. A. Lampert, *Physical Review*, 1956, **103**, 1648-1656.